Proceedings of the ASME 2021 17th International Manufacturing Science and Engineering Conference
MSEC2022
June 27-July 1, 2022, West Lafayette, Indiana, USA

MSEC2022-85745

EFFECT OF WITHDRAWAL VELOCITY ON PARTICLE ENTRAINMENT FROM DENSITY MISMATCHED MIXTURE

S M Naser Shovon
Dept. of Mechanical Engineering
University of Maine
Orono, ME

Ibrahim Khalil,
Dept. of Mechanical Engineering
The University of Maine
Orono, ME

Adeeb Alam,
Dept. of Mechanical Engineering
The University of Maine
Orono, ME

Bashir Khoda, Ph.D.*
Dept. of Mechanical Engineering
University of Maine
Orono, ME

ABSTRACT

In this work, the physical phenomenon of the polydisperse micro-particle entrainment process from density mismatch mixture is investigated with the variation of substrate withdrawal speed. A liquid carrier system (LCS) is prepared by a polymer-based binder and an evaporating solvent. Nickel-based inorganic and spherical particles with a. moderate vol%. of 35% are added to the LCS solution. The cylindrical AISI 1006 mild steel wire substrate is dipped at different withdrawal speed ranging from 0.01 mms-1 to 20 mms-1. The binder vol%. is varied between 6.5% and 10.5%. Once the cylindrical substrate is extracted from the mixture, the surface coverage and the particle size are measured following the image analysis technique. The average particle size, coating thickness and the surface packing coverage by the particles are increasing with the higher withdrawal speed of the substrate. We observed relatively low size of particles (<10 micrometers) as well as low surface coverage (~33%) when the withdrawal speed remains at 0.01 mm/s. However, with high withdrawal speed (20 mm/s), we found all sizes of particles present on the substrate with a surface coverage of over 90%. The finding of this research will help to understand the high-volume solid transfer technique and develop a novel manufacturing process.

NOMENCLATURE

U	withdrawal speed
ϕ_s	solvent volume fraction
ρ_s	density of LCS solution
ρ_{sv}	density of solvent
ρ_b	density of binder
ϕ_b	binder volume fraction
ϕ_p	particle volume fraction
ϕ_s	solvent volume fraction

1. INTRODUCTION

Higher yield particle transfer during dip coating can be crucial to address current challenges facing the manufacture of next-generation materials and devices [1]. The dipping mixtures can be embedded with inorganic fillers, nanoparticles, or microparticles and their solid loading can reach up to the jammed state (64%). Adding larger inorganic particles (>1μm), however, will result in a multi-phase negatively buoyant mixture which is difficult to control, and it becomes challenging to transfer particles from the mixture. The deposition of a specific material in liquid phase (solution) or solid phase (powder or nanoparticles) [2] on a substrate is a standard process in everyday life and industrial applications [3]. Coating processes are now extensively used in widespread applications of radio frequency identification [4], batteries [5], sensors [6], organic photovoltaics [6], fuel cells [7], e-paper [8], microfluidics [9, 10] and super-capacitors [11, 12] due to their thin layer formation. In such situations, the control over the coating regime becomes important and it initially depends on the target substrates (wires, plates or fibers), process parameters and the uniformity of coating layer.

Suspension of solid particles has become very popular for its numerous applications in industrial process including the coating of surfaces, the cleaning of substrate or the dispensing of liquid. Considering its abundant application, the complex behavior of suspensions has received substantial attention in past. Several studies have described the suspension rheology [13], clogging in confined flows [14, 15] or the inertial suspension flow [16]. However, the complexity of density-mismatched high solid concentrated suspension behavior during a dip coating process is not fully captured in recent studies.

Earlier particle transfer by dip coating has been investigated for monolayer formation of nanoparticles or process parameters (i.e. dipping angle, withdrawal speed, immersion time etc) influence on the deposited layer. The effect of withdrawal speed on the dip

coated layer has been investigated before both in large microparticles or nano particles. Núñez *et al.* [17] investigated the influence of withdrawal speed (0.1 – 10 μm/s) on monodisperse silica spheres (100 nm to 1 μm dia.) for self-assembly monolayers (SAMs) formation through dip coating process. Wang *et al.* [18] also investigated the SAMs formation with silica spheres (2 μm dia.) changing the withdrawal speed from 0.11 to 5.35 mm/s. Large microparticles transfer from dip coating are also investigated before. Gans *et al.* [19] investigated polystyrene particles (40, 80, 140, 250 μm) in a suspension by changing the withdrawal speed from 24 to 1453 μm/s. Similarly, Palma *et al.* [20] analyzed a particulate suspension of polystyrene particles (80, 145 or 550 μm) in different withdrawal velocity (0.03 to 13 mm/s). The significance of using binder in dip coating process was also described in microparticles transfer before. *Hemra et al.* used latex binder including acrylic emulsion, poly vinyl alcohol (PVA) and polyethylene oxide (PEO) for preparing micro-porous alumina membrane with alumina powder in the dip coating of alumina tube [21]. *Varga et al.* also used polyurethane binder for dip coating α-Al_2O_3 ceramic particles (0.3 and 2 μm) in a polyamide fiber [22]. However, most of the articles investigated the nano or microparticle suspension of neutrally buoyant mixture. The influence of withdrawal velocity in dip coating process from density mismatch mixture is not reported before.

In this work, density mismatched heterogeneous mixture is prepared with polymer binder, solvent and inorganic polydisperse micro-particles (~1 to 20 μm). An external kinetic energy is provided into the mixture to create a pseudo suspension. Cylindrical rod is used as dipping substrate to investigate the solid transfer process from complex mixture with the variation of substrate withdrawal speed. We experimentally studied the influence of withdrawal speed on the particle transfer process and compare the coating thickness, entrained particle size and the surface coverage.

2. MATERIALS AND METHODS

The density mismatched mixture has two part (i) a liquid carrier system (LCS) and (ii) the transferrable particles. The LCS contains Polymethyl Methacrylate (PMMA) as the binder and 1,3-Dioxolane as the solvent. The binder has a molecular weight of ~15000 g/mol, low density (~1.19 g/cm^3) and 41 mN/m surface tension. The solvent has 1.06 g/cm^3 density, 34.3 mN/m surface tension, 78 °C boiling point, and 79 mmHg vapor pressure at 20°C. Both components are acquired from Sigma Aldrich which are mixed in room temperature and stirred for 2 hours. Nicrobraz 51 (Cr 25%, P 10% and Ni Bal.), acquired from Wall Colomonoy, is considered as the transferrable particles. The average particle diameter from the supplier is 44 μm and it exhibits spherical morphology. The particles are sieved with Gilson Performer III shaker through Stainless Steel 635 mesh (20 μm) in our lab to reduce polydispersity and particle size distribution is discussed our previous article [23]. After repeated sieving the average particle diameter is measured at 5.69 μm, with standard deviation of 3.19.

Particles are added gradually into the LCS solution to create the mixture. Due to their huge density differences (>7), the particles sediment quickly and creating a negative buoyant mixture. To ensure the homogeneity and avoid sedimentation of particles, the mixture is stirred with minimal suspending speed (~600 rpm) during dipping the substrate which creates a pseudo suspension. Mild steel of AISI 1006 with 1.06 mm dia. is considered for transferring the solid particles. The wires are cleaned in an ultrasonic bath for 30 minutes at 50 °C for removing surface contaminant and passive film. The mixture height was 1 inch, and the dipping length of the rod was 0.6 inch considering the clearance for rotating stirrer. A fixed 35% powder volume fraction is used in this investigation to determine the effect of withdrawal speed. It should be noted that >25 vol%. of particles create a concentrated mixture. Two polymeric binder vol%. (6.5% and 10.5%) is used in our experiment which are defined as low and high binder concentration as shown in Table 1.

An in-house dipping station is prepared for this work shown in figure 1. The dipping setup controls the withdrawal speed, U and the immersion time of the substrate using a numerical control system. The experiments are performed within low to high range of withdrawal speed, $U \in [0.01, 20]$ mms^{-1} and a fixed 10 second immersion time. The setup is maintained at 25 °C room temperature and 20% relative humidity. The dipping experiments were done instantly after making the pseudo suspension to minimize the evaporation of solvent during experiment. Also, the mixture is contained in an air tight jar at interim period to reduce the solvent evaporation. After withdrawal, the rod is dried for 4-6 hours in room temperature and then images are taken for analysis. The surface images from top, middle and bottom of the dipped portion of substrates are taken using VHX 7000 Digital 4K microscope (KEYENCE Corporation Ltd., IL). High resolution 4K images are analyzed in MATLAB using image analysis script. The MATLAB code calculated the pixel size of each particle in the images and identify the closed loop for particle count. The length scale is converted from pixel size to count the average particle size and surface coverage. The coating thickness was measured three times from the difference of coated and uncoated rod dia. in three different locations (top, middle and bottom) of the dipped substrate.

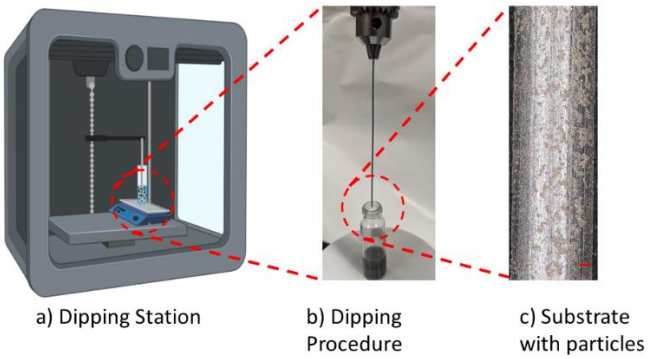

Figure 1:Schematic diagram of the dipping station and dipping procedure. The scale bar is for 50 μm.

3. RESULTS AND DISCUSSION

We started characterizing the microscopic structure of the coating layer investigating the withdrawal speed on the solid transfer. Adding binder and immiscible particles to any liquids transforms its original physical properties e.g., density, viscosity. The modified suspension density is measured using the following equation: $\rho_s = \rho_{sv} + (1 - \phi_s)\rho_b$, where ϕ, and ρ_s denote for surface tension, volume fraction, and density of LCS solution, ϕ_s for solvent volume fraction, and the subscript sv and b denotes solvent and binder, respectively. LCS is the particle bearing fluid which exhibited a Newtonian rheological behavior in different volume fraction. Increasing the binder increase the viscosity of the LCS, which been tested by our Rheometer and the data has been presented in our prior work [24].The addition of particles will act as obstacles to the fluid flow which may induce non-Newtonian behavior. Similarly adding binder will also increase the viscosity which may facilitate to adhere the particles on the surface of the substrate.

Table 1: Composition of binder, particles and solvent in 7ml density mismatch mixture

Composition Name	VF (%) of binder, particles and solvent		
	Binder (ϕ_b)	Particles (ϕ_p)	Solvent (ϕ_s)
Low Binder	6.5	35	58.5
High Binder	10.5	35	54.5

We performed the dipping experiments in six different withdrawal speeds including 0.01, 0.1, 1, 5, 10 and 20 mms^{-1} at both low and high binder concentration. We observed two different regimes including (i) heterogeneous regime and (ii) effective viscous regime in different withdrawal speed. In 20 mms^{-1} and 10 mms^{-1}, dipping in high binder mixture generates effective viscous regime on the substrate transferring higher volume of material. However, dipping in low binder mixture even at higher speed (20 mms^{-1} and 10 mms^{-1}) transfers relatively lower volume of material introducing heterogeneous regime on the substrate. In lower withdrawal speed (<10 mms^{-1}) both of the composition follows heterogeneous coating regime.

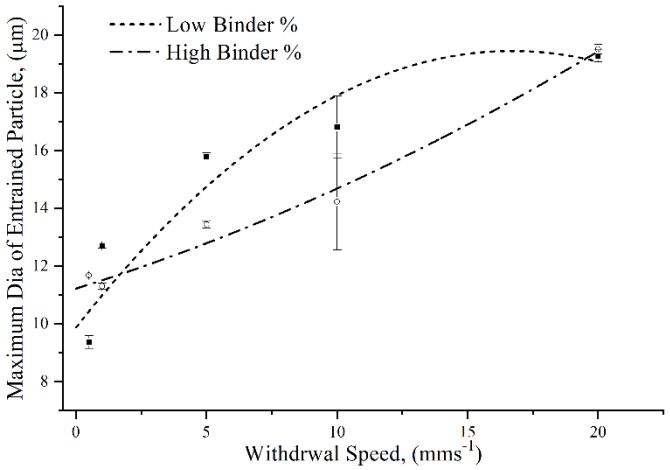

Figure 2:Schematic diagram of maximum particle size vs withdrawal speed.

Table 2: Maximum particle size and surface coverage on different withdrawal speed and capillary number.

Composition Name	Withdrawal Speed, U (mms^{-1})	Coating Thickness (μm)	Maximum Particle size (μm)	Avg. Surface coverage by particles
High Binder	20	43.37	19.51	95.18%
High Binder	10	29.53	14.23	84.69%
High Binder	5	11.94	13.44	66.50%
High Binder	1	12.87	11.30	49.51%
High Binder	0.5	13.4	..	..
High Binder	0.1	..	11.68	43.38%
High Binder	0.01	..	10.73	40.67%
Low Binder	20	15.44	19.28	66.81%
Low Binder	10	15.39	16.81	63.85%
Low Binder	5	9.06	15.79	52.42%
Low Binder	1	5.25	12.70	50.65%
Low Binder	0.5	2.79	..	..
Low Binder	0.1	..	9.37	34.63%
Low Binder	0.01	..	8.61	30.63%

In heterogeneous regime, the particle entrainment varies with different withdrawal speed. When U becomes low, the maximum particle size entrainment, coating thickness and surface coverage becomes smaller shown in figure 2,3 and 4. For example, we observed in maximum 10.73 μm particle in high binder concentration and 8.61 μm particle in with low binder mixture at 0.01 mms^{-1}. The solvent evaporation becomes faster, and the

liquid film becomes thinner in low withdrawal speed. Also, the convective influx of particles becomes limited with the influence of solvent evaporation in low withdrawal speed [25]. Thus, thin liquid film cannot facilitate large size of particles in low withdrawal speed and the maximum particle size becomes smaller in low capillary number.

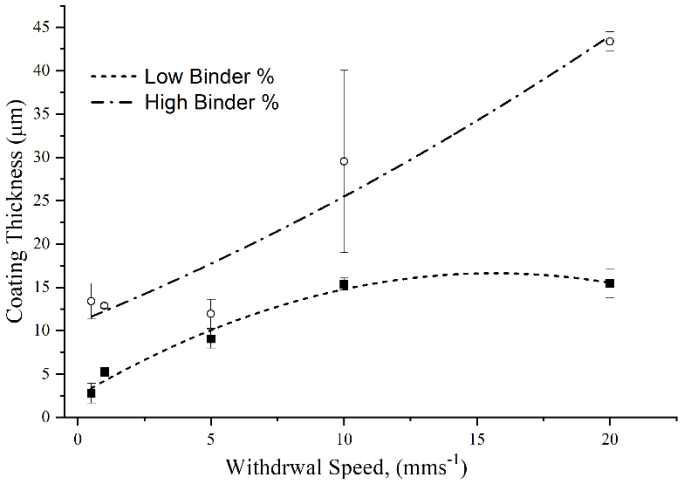

Figure 3:Schematic diagram of thickness vs withdrawal speed.

Similarly, we found low coating thickness in smaller speed below 10 mms^{-1} and the particle laden film contains mostly single-layer film formation there. However, in withdrawal speed 10 mms^{-1} and over, low binder mixture provides 15.39 μm and 15.44 μm coating thickness in 10 and 20 mms^{-1} respectively. As we are using polydisperse microparticles ranging from 1 to 20 μm, it can be predicted that the film formation in low binder mostly follows single-layer accumulation. However, at high binder, we found higher coating thickness of 29.53 μm and 43.37 μm at withdrawal speed of 10 and 20 mms^{-1} respectively. This coating thickness is higher than the polydisperse particle range used in the pseudo suspension. Thus, the multi-layer coating film formation can be demonstrated from high binder in 10 and 20 mms^{-1} withdrawal speed. In high binder, we increased the polymer content in the LCS which increases the viscosity of the LCS as well as the pseudo suspension. Moreover, in high withdrawal speed of 10 and 20 mms^{-1}, high viscous fluid flows towards the substrate with higher influx of particles which dominates more than the variation of withdrawal speed and facilitate the entrainment of particle and makes an effective viscous regime.

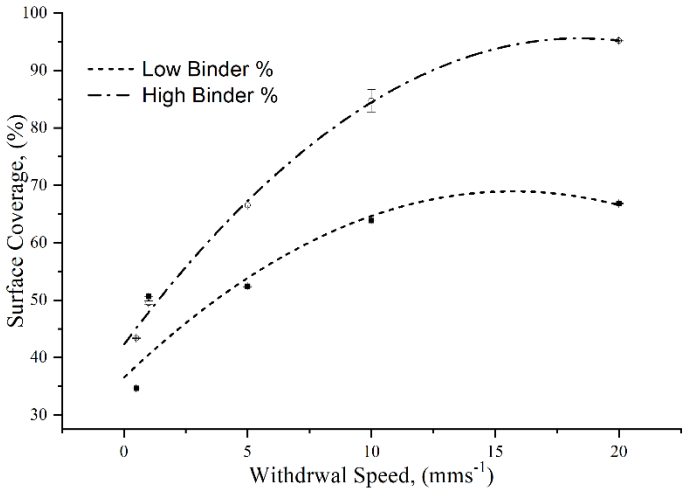

Figure 4:Schematic diagram of surface coverage vs withdrawal speed.

At lower binder concentration, we observed heterogeneous regime with high withdrawal speed ($U \geq 10$ mms^{-1}) shown in Figure 5. The low polymer content in low binder mixture provides lower adhesion to the particles which makes the surface coverage lower by particles and makes a heterogeneous particle entrainment. We found in maximum 66.81% coverage by particles in 20 mms^{-1} withdrawal speed shown in figure 4.

We observed effective viscous regime in high binder concentration only when withdrawal speed, $U \geq 10$ mms^{-1}. The polymer content increases the viscosity of the LCS as well as the particle laden liquid mixture. In high binder mixture, the polymer content becomes higher which facilitates more adhesion of particles on the substrate. Moreover, with high withdrawal speed, the solvent evaporation becomes slower, and more liquid is adhered on the substrate. This liquid contains more particles due to the high convective influx of particles at larger withdrawal speed. Also, the polymer content inhabits higher liquid film thickness and high viscosity which also provides enough adhesion and contact area for large size of particles [26]. We observed 95.18% surface coverage by particles and 19.51 μm size of particle in 20 mms^{-1} withdrawal speed with high concentration of binder.

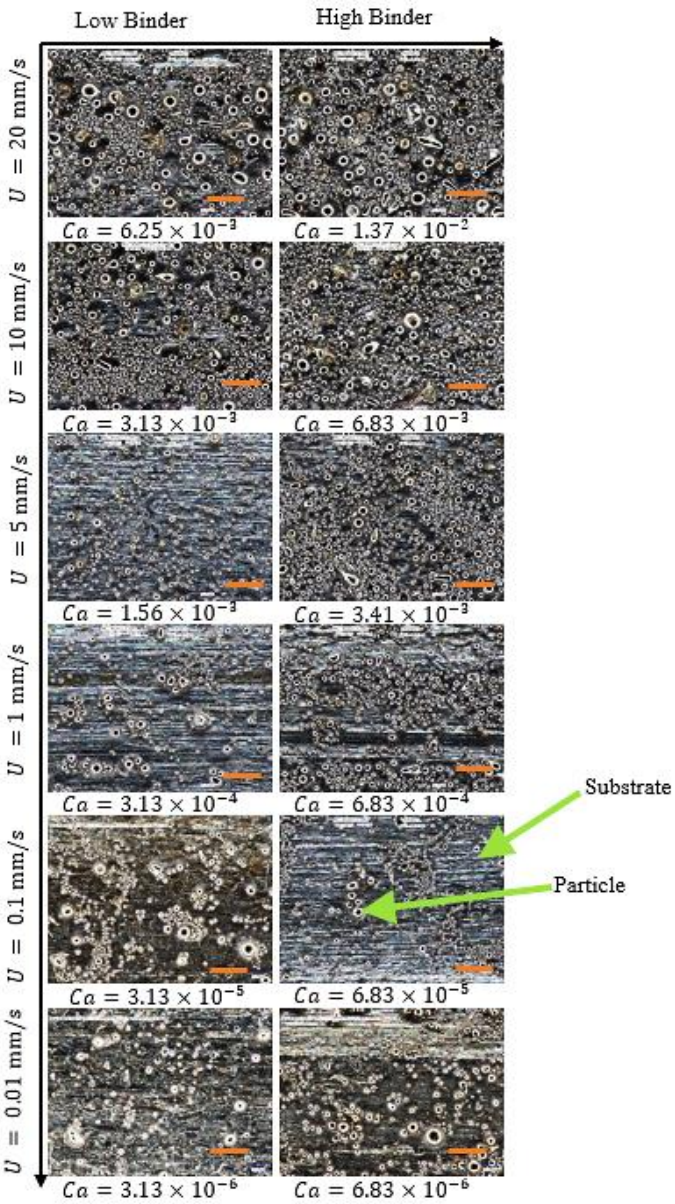

Figure 5: Effect of withdrawal velocity in low binder and high binder concentration. The scale bar is for 50 µm.

4. CONCLUSION

We have investigated the influence of substrate withdrawal speed on the particle entrainment for an efficient solid particle transfer process. Analyzing the surface packing coverage and maximum particle size, we have demonstrated that different size of particles can be separated in a fixed composition of binder and particles by varying the withdrawal speed. We can separate small size of particles (< 10 µm) by using 0.1 mms^{-1} and 0.01 mms^{-1} withdrawal speed at lower concentration of binder. In future, we will characterize the process parameters of dip coating to achieve high potentiality and cost-effective output from this process. Investigating the effect of evaporation and particle sorting process with the variation of the viscosity will be our future work.

ACKNOWLEDGEMENTS

The authors thank Alex Watson and John Belding, Director of Advanced Manufacturing Center (AMC) for helping with the microscopy. Financial supports from Grant NSF-CMMI # 2101751, US-DOT # 693JK31850009CAAP and UMaine-NEU Seed Grant are acknowledged.

REFERENCES

1. Khoda, B., et al., *3D metal lattice structure manufacturing with continuous rods.* Scientific Reports, 2021. **11**(1): p. 434.
2. Sajid, M., et al., *Highly stable flex sensors fabricated through mass production roll-to-roll micro-gravure printing system.* Sensors and Actuators, A: Physical, 2015.
3. Ruschak, K.J., *Coating flows.* Annual Review of Fluid Mechanics, 1985. **17**(1): p. 65-89.
4. Ghosh, S.K., *Functional Coatings and Microencapsulation: A General Perspective*, in *Functional Coatings*. 2006. p. 1-28.
5. Krebs, F.C., *Fabrication and processing of polymer solar cells: A review of printing and coating techniques.* Solar energy materials and solar cells, 2009. **93**(4): p. 394-412.
6. Liang, R., et al., *Microcup® displays: Electronic paper by roll-to-roll manufacturing processes.* Journal of the Society for Information Display, 2003. **11**(4): p. 621-628.
7. Nanjundaswamy, K.S., et al. *Electrode fabrication for Li-ion: processing, formulations and defects during*

coating. in *IECEC-97 Proceedings of the Thirty-Second Intersociety Energy Conversion Engineering Conference (Cat. No. 97CH6203)*. 1997. IEEE.
8. Choi, E.K., et al., *Fabrication of electrodes and near-field communication tags based on screen printing of silver seed patterns and copper electroless plating.* International Journal of Precision Engineering and Manufacturing, 2015.
9. Son, J.M., et al., *Temperature distribution measurement of Au micro-heater in microfluidic channel using IR microscope.* International Journal of Precision Engineering and Manufacturing, 2015.
10. Prakash, S. and S. Kumar, *Fabrication of microchannels on transparent PMMA using CO2 Laser (10.6 μm) for microfluidic applications: An experimental investigation.* International Journal of Precision Engineering and Manufacturing, 2015.
11. Yu, J.H., et al., *Electrical behavior of laser-sintered Cu based metal-organic decomposition ink in air environment and application as current collectors in supercapacitor.* International Journal of Precision Engineering and Manufacturing - Green Technology, 2015.
12. Karakaya, M., et al., *Roll-to-roll production of spray coated N-doped carbon nanotube electrodes for supercapacitors.* Applied Physics Letters, 2014.
13. Zarraga, I.E., D.A. Hill, and D.T. Leighton Jr, *The characterization of the total stress of concentrated suspensions of noncolloidal spheres in Newtonian fluids.* Journal of Rheology, 2000. **44**(2): p. 185-220.
14. Sauret, A., et al., *Clogging by sieving in microchannels: Application to the detection of contaminants in colloidal suspensions.* Applied Physics Letters, 2014. **105**(7): p. 074101.
15. Dressaire, E. and A. Sauret, *Clogging of microfluidic systems.* Soft Matter, 2017. **13**(1): p. 37-48.
16. Matas, J.-P., J.F. Morris, and É. Guazzelli, *Inertial migration of rigid spherical particles in Poiseuille flow.* Journal of Fluid Mechanics, 2003. **515**: p. 171-195.
17. García Núñez, C., et al., *Large-Area Self-Assembly of Silica Microspheres/Nanospheres by Temperature-Assisted Dip-Coating.* ACS Applied Materials & Interfaces, 2018. **10**(3): p. 3058-3068.
18. Y.Wang, et al., *Large-area self assembled monolayers of silica microspheres formed by dip coating.* Materials science-poland, 2010. **28**(2).
19. Gans, A., et al., *Dip-coating of suspensions.* Soft matter, 2019. **15**(2): p. 252-261.
20. Palma, S. and H. Lhuissier, *Dip-coating with a particulate suspension.* Journal of Fluid Mechanics, 2019.
21. Hemra, K., P. Aungkavattana, and D. Atong. *Micro-porous alumina membrane prepared by dip coating using latex binder*. in *Materials Science Forum*. 2011. Trans Tech Publ.
22. Varga, K., F.A. Reifler, and F. Clemens. *Dip coating of fibers with ceramic particles*. in *37th International Symposium on novelties in Textiles, Ljubljana, Slovenia*. 2006.
23. Khoda, B., A.M.M. Nazmul Ahsan, and S.M.N. Shovon. *Solid Transfer of Large Particles by Dipping in a Heterogeneous Mixture*. in *ASME 2021 16th International Manufacturing Science and Engineering Conference*. 2021.
24. Khoda, B., A.M.M.N. Ahsan, and S.M.N. Shovon, *Dip Coating From Density Mismatching Mixture.* Journal of Micro and Nano-Manufacturing, 2021. **9**(2).
25. Brinker, C.J., *Dip coating*, in *Chemical Solution Deposition of Functional Oxide Thin Films*. 2013.
26. Khalil, I. and B. Khoda, *Sorting of Poly-Disperse Particle by Entrapment Using Liquid Carrier System.* Journal of Manufacturing Science and Engineering, 2021. **144**(5).